4 January 2002

Chemical Physics Letters 351 (2002) 142 148

CHEMICAL PHYSICS LETTERS

www.elsevier.com/locate/cplett

Determination of the electron localization function from electron density

Vladimir Tsirelson [a,*], Adam Stash [b]

[a] *Mendeleev University of Chemical Technology, Miusskaya Sq. 9, 125047 Moscow, Russia*
[b] *Karpov Institute of Physical Chemistry, ul. Vorontsovo pole 10, 103064 Moscow, Russia*

Received 7 September 2001; in final form 2 November 2001

Abstract

Approximate determination of electron localization function (ELF) from electron density and its first and second derivatives is described. It is demonstrated that the second order gradient expansion of the kinetic energy density yields the modified ELF, which exhibits all the features characterizing electron pairing. Calculations based on the accurate electron densities derived from X ray diffraction data carried out for crystalline magnesium oxide, chlorine and urea: they demonstrate that the ELF reveals important peculiarities of crystal architecture. © 2002 Elsevier Science B.V. All rights reserved.

1. Methodology and results

The purpose of this Letter is to demonstrate that electron localization function (ELF) introduced by Becke and Edgecombe [1] and extensively studied over the last few years [2 7] can be approximately derived from the electron density, e.g., the experimental electron density measured in the accurate X-ray (or synchrotron) diffraction experiment [8]. The arguments favouring ELF as a tool illustrating the bonding theory are as follows [1]. The spatial localization of electron pairs in atoms, molecules and crystals is described by the pair probability of finding an electron in the vicinity of another (reference) electron with the same spin and its associated Fermi hole function [9,10]. The latter directly reflects the effect of the Pauli exchange repulsion of electrons with parallel spins. The leading term in the Taylor expansion of spherically averaged conditional parallel-spin pair probability in a system described by a single-determinant wave function turns out to be proportional to the positive function of electron kinetic energy density [11]

$$D_\sigma(\mathbf{r}) = \sum_i \nabla\varphi_i(\mathbf{r})\nabla\varphi_i(\mathbf{r}) - (1/4)|\nabla\rho_\sigma(\mathbf{r})|^2/\rho_\sigma(\mathbf{r}), \quad (1)$$

where $\varphi_1(\mathbf{r})$ are the Hartree Fock orbitals, $\rho_\sigma(\mathbf{r})$ is the density of the σ-spin electrons in the system under consideration (sum runs over the σ-spin orbitals). The smaller is the probability, the

* Corresponding author. Fax. +7 095 200 4204.
E mail address: tsirel@muctr.edu.ru (V. Tsirelson).

0009 2614/02/$ see front matter
PII: S0009 2614(01)01361 6

higher is a localization of the reference electron. That is why the D_σ is low in the regions of high electron pair localization as the core electron shells and bonding and electron lone pairs in molecules and crystals. To extract the information regarding the spatial electron localization from the kinetic energy density. Becke and Edgecombe [1] introduced a dimensionless scalar ELF

$$\eta = [1 + (D_\sigma/D_{\sigma,0})^2]^{-1}. \tag{2}$$

The term

$$D_{\sigma,0}(\mathbf{r}) = (3/5)(6\pi^2)^{2/3}[\rho_\sigma(\mathbf{r})]^{5/3} \tag{3}$$

describes the kinetic energy density of a homogeneous electron gas with the spin density locally equal to $\rho_\sigma(\mathbf{r})$. The values of ELF (2) are restricted to $0 \leqslant \eta \leqslant 1$, value $\eta = 1$ corresponds to complete electron pair localization, $\eta = 1/2$ represents a homogeneous electron gas-like pair probability (electron delocalization), and η close to zero denotes the borders between electron pairs.

Eq. (3) for the closed-shell systems can be rewritten [2,3]

$$\eta = \left[1 + (D_P/D_0)^2\right]^{-1}. \tag{4}$$

Here

$$D_P = t(\mathbf{r}) - (1/8)|\nabla\rho(\mathbf{r})|^2/\rho(\mathbf{r}) \tag{5}$$

is so-called Pauli kinetic energy [12,13] ($\rho(\mathbf{r})$ is the total electron density) and

$$t(\mathbf{r}) = (1/2)\sum_i \nabla\varphi_i(\mathbf{r})\nabla\varphi_i(\mathbf{r}) \tag{6}$$

is the kinetic energy density (the summation is performed over all the occupied orbitals) and

$$D_0(r) = (3/10)(3\pi^2)^{2/3}[\rho(\mathbf{r})]^{5/3} \tag{7}$$

is the kinetic energy density of a homogeneous electron gas with the density locally equal to the total electron density $\rho(\mathbf{r})$.

To avoid the necessity to calculate ELF from one-electron wave functions, let us replace (6) by the second-order gradient expansion of the kinetic energy density [14]

$$t_{DFT}(\mathbf{r}) = (3/10)(3\pi^2)^{2/3}[\rho(\mathbf{r})]^{5/3} + (1/72)|\nabla\rho(\mathbf{r})|^2/\rho(r) + (1/6)\nabla^2\rho(\mathbf{r}). \tag{8}$$

The latter (Kirzhnits) approximation used in the density functional theory (DFT) [15] is suitable for the case of the smooth (but not necessary small) variation of the electron density. It allows rewriting the Eq. (5) as

$$D_{P,DFT} = (3/10)(3\pi^2)^{2/3}[\rho(\mathbf{r})]^{5/3} - (1/9)|\nabla\rho(\mathbf{r})|^2/\rho(\mathbf{r}) + (1/6)\nabla^2\rho(\mathbf{r}). \tag{9}$$

Thus, the expression for ELF takes the form

$$\eta_{DFT} = \left[1 + (D_{P,DFT}/D_0)^2\right]^{-1}, \tag{10}$$

i.e. η_{DFT} turns out to be dependent only on the electron density and its derivatives.

The asymptotic behaviour of the functions D_σ and D_0 with $\mathbf{r} \to \mathbf{R}_i$ [11] indicates that exact ELF (2) goes to 1 in the vicinity of the nuclei at $\mathbf{R}_i$, while the approximate ELF (10) approaches to zero in these regions due to a discontinuity of the Laplacian term in (9) at $\mathbf{r} = \mathbf{R}_i$. Additionally, the approximate function $D_{P,DFT}$ becomes negative near the nuclei. Therefore, the regions around the nuclei should be omitted. It is worth noting that the accuracy of determination of both experimental and theoretical electron densities close to the nuclei is not accurate due to a variety of factors [8]. Long-range behaviour of the ratios $D_\sigma/D_{\sigma,0}$ and $D_{P,DFT}/D_0$ provides the vanishing of the ELF (2) and (10) in finite systems when $\mathbf{r} \to \infty$; it is in agreement with an asymptotic behaviour of the electron density itself [16]. We did not observe the deviations from such behaviour as it was noted for atoms in [2].

Comparison of the ELF functions for Ne atom calculated with help of the expressions (2) and (10) is given in Fig. 1 (wave functions were computed by non-empirical Hartree Fock method in the 6-31G basis set). Fig. 1 demonstrates that ELF in the DFT approximation (10) reveals the electronic shell structure of the Ne atom. The minima of η and η_{DFT} denoting the K-shell radius [6] are in

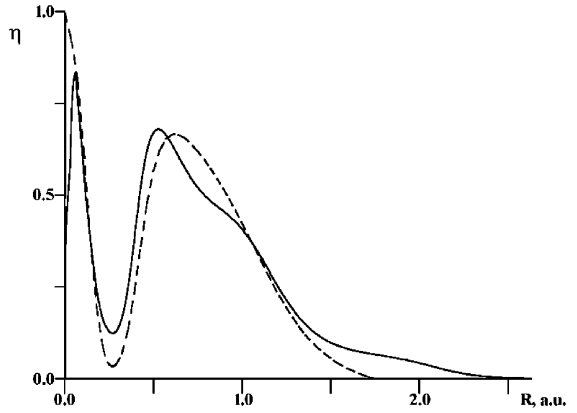

Fig. 1. Electron localization functions for Ne atom: η calcu lated by expression (2) is depicted by dashed line, while η_{DFT} calculated by expression (10) is shown by the solid lines. Non empirical Hartree Fock wave functions computed with 6 31G basis set have been used in calculations.

excellent agreement: though the shape of the approximate ELF η_{DFT} differs somewhat from η in the valence region, all the main features seems to be reproducible. Calculations carried out for other atoms yielded a similar result [17]. These calculations have also shown that approximate ELF η_{DFT} possesses the same specific feature as initial η (2) [2]: η_{DFT} has a value close to 1 over the atomic basin of H and He atoms excluding the nearest vicinity of the nuclei.

Thus, the approximate ELF determined from the electron density possesses all the features characterizing the electron pairing. Let us now discuss the specificity of the ELF determination from the experimental electron density. Modern single-crystal X-ray and synchrotron diffraction methods allow measuring the diffracted intensities with accuracy of about 1% [8]. After correcting the measured intensities for multiple scattering, thermal diffuse scattering, absorption and extinction, the electron density of a crystal can be reconstructed by the fit of the multipole structural model to the structure factors [8]. Model quasi-static electron density only slightly suffers from random and model errors as limited resolution and incomplete thermal deconvolution and, although it is not derived from the variational principle and does not obeys the local virial theorem, it is close to the quantum mechanical electron density. The model electron density provides also the kinetic energy density, as approximated by (8), which is in very reasonable agreement with their Hartree Fock analogue for the molecules and crystals with different types of the chemical bond [18]. Therefore we tested the possibility of the use of the ELF η_{DFT} determined using the experimental model electron density, to reveal the regions of the electron pair localization in crystals. Corresponding maps of the ELF η_{DFT} for crystalline MgO, chlorine and urea are presented in Figs. 2 4.

Gradient expansion (8) used in this work to approximate the kinetic energy density $t(\mathbf{r})$ is not the only one available: the other approximations have also been suggested [15]. However, the Weizsacker approximation

$$t_W(\mathbf{r}) = (3/10)(3\pi^2)^{2/3}[\rho(\mathbf{r})]^{5/3} + (1/8)|\nabla\rho(\mathbf{r})|^2/\rho(\mathbf{r})$$

[19] yields $\eta = 1/2$ everywhere in space, while Yang approximation [20]

$$t_Y(\mathbf{r}) = (3/10)(3\pi^2)^{2/3}[\rho(\mathbf{r})]^{5/3} + (1/72)|\nabla\rho(\mathbf{r})|^2/\rho(\mathbf{r}) + (1/12)\nabla^2\rho(\mathbf{r}),$$

as we have found, gives worse description of the atomic cores. It is well known that no DFT approximation for $t(\mathbf{r})$, which is capable of providing a good description over the entire range of values of $\mathbf{r}$ [11,15]. That is a consequence of rapid variation of the electron density in the vicinity of the nuclei and its slow variation in the valence electron shells. Kirzhnits approximation (8) provides a compromise solution giving an acceptable local behaviour of the approximate ELF over all the position space excluding small areas surrounding the nuclei. At the same time, the case of urea (Fig. 4) reveals the shortcoming of the approximate ELF: it has the double peak along the covalent bonds, while accurate Hartree Fock wave function-based ELF does not. This artifact is a consequence of the deficiency of gradient expansion of the kinetic energy density (6).

Note that there is another approach to determine the ELF beyond the orbital approximation

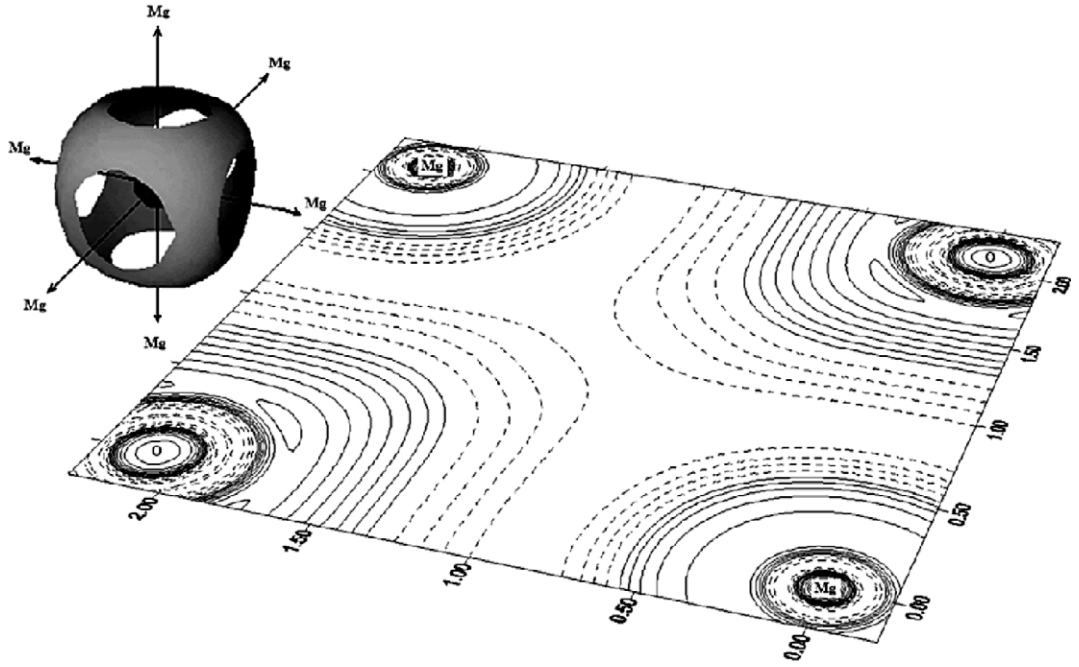

Fig. 2. Electron localization function η_{DFT} in the (1 0 0) plane of MgO. Solid lines correspond to values $\eta_{DFT} \geqslant 0.5$ (line interval is 0.05), while broken lines correspond to values $\eta_{DFT} < 0.5$ (line interval is 0.10). Envelope surface of $\eta_{DFT} = 0.86$ around the O ion is also shown.

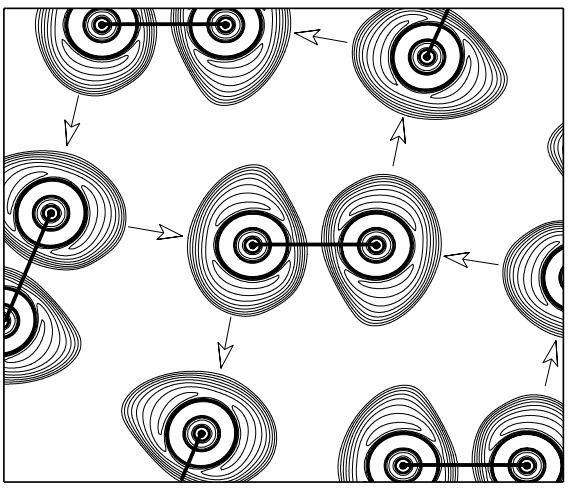

Fig. 3. Electron localization function η_{DFT} in the plane (0 0 1) of crystalline Cl_2 (parameters of the multipole model of electron density are taken from [29]). Only lines correspond to values $\eta_{DFT} \geqslant 0.5$ are shown with the line interval of 0.05. Thick lines connect atoms within Cl_2 molecules, while the arrows indicate the 'key and lock' intermolecular interactions.

[21]. It is based on the virial theorem-relationships derived in the DFT and allows expressing ELF in terms of the exchange energy density, electron density, its Laplacian and gradient of the electrostatic potential. Unfortunately, in this approach D_P (5) depends on the position of origin of the coordinate system making the ELF study for molecules and crystals more difficult.

2. Discussion

Consideration of Laplacian of the electron density [10] is often used to reveal the charge density concentrations empirically associated with the number and spatial arrangement of the localized electron pairs assumed in the VSEPR model [22]. More strictly, the spatial distribution of electron pairs is described by a six-dimensional pair probability function [9]. The Pauli principle leads to the partition of the space of a many-electron system into the regions occupied by the

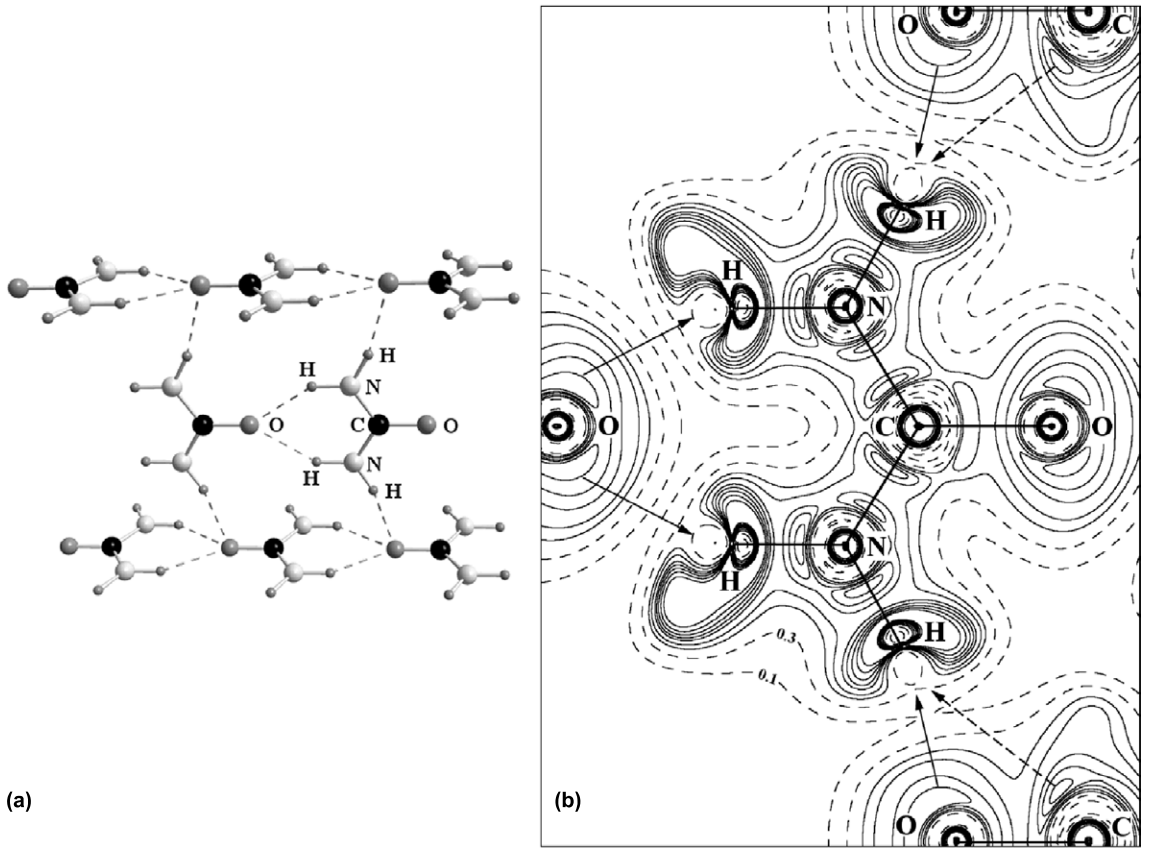

Fig. 4. Mutual molecular arrangement (a) and electron localization function η_{DFT} in the plane (1 1 0) of crystalline urea (b); multipole parameters describing the electron density are taken from [33]. Solid lines correspond to values $\eta_{\mathrm{DFT}} \geqslant 0.5$ (interval is 0.05), dashed lines are specified in the map. Solid arrows show the hydrogen bonds, while the dashed arrows indicate the secondary intermolecular interactions of the 'key and lock' type. The negative areas around the hydrogen positions are not shown.

pairs of electrons with opposite spins [23–26]. Being a measure of the excess of the local kinetic energy due to Pauli's repulsion, ELF allows mapping the implicit features of such a partitioning onto a position space. Moreover, the topological analysis of $\eta(\mathbf{r})$ [4,5] exhibits the existence of the bonding, non-bonding and core attractors (local maxima in the ELF) surrounded by their corresponding space domains. The number and spatial arrangement of these attractors provides a basis for classification of the chemical bonds [4,5,7], while quantitative characteristics of the domains describe specific features of these bonds [27,28].

Consider now the examples of ELF (10) determined from the experimental electron density. Crystalline MgO is usually considered as an example of an ionic chemical bond characterized by the electron density shift from the cation to anion. Fig. 2 reveals significant electron localization around the bonded ions, the electron concentration around oxygen being larger in size. The valence electron shell of each anion is non-spherical and has six well-defined attractors ($\eta_{\mathrm{DFT}} = 0.86$) aligned with the [1 1 1] and symmetry equivalent directions. This is in good agreement with the ELF pattern of NaCl obtained by LMTO calculation [7].

The crystal structure of Cl_2 (space group Cmca) is layered with all the atoms in the planes parallel to (1 0 0). Each Cl atom is linked by the bond paths, lines of maximum electron density, to three atoms belonging to the neighbour molecules in the same layer, two intermolecular contacts have

lengths of 3.28 Å, which are significantly less than doubled van der Waals radius of 1.8 Å. Fig. 3 reveals that electron pairs in Cl_2 are concentrated in the atomic basins. It is remarkable that a lone-pair of each Cl atom faces an ELF hole of another atom in the same layer. Each atom is involved in two interactions of this kind: as a Lewis base in one case and as a Lewis acid in the another. In terms of the topological analysis [4,5], we can say that a non-bonding ring attractor of one Cl atom interacts with an axial (3,+1) critical points of another. These two-dimensional directional 'key-and-lock' interactions in the (1 0 0) plane of solid chlorine provide a specific mutual arrangement of molecular units Cl_2 with the short nearest-neighbour inter-molecular contacts minimizing the energy of molecular interactions in a crystal.

This agrees very well with the result of the analysis of the Laplacian of the electron density [30]. The latter analysis also reveals the directional interactions resulting from the alignment of non-bonded electron density concentrations on one of Cl atoms with the electron density depletions on another. This observation reflects a similarity between imaging the electron localization via the ELF and Laplacian fields, as stressed in [5]. The homeomorphism of these two fields was also reported in recent study of three-dimensional directional S···N interactions taking place between S_4N_4 molecules in a crystal [31].

The case of urea $CO(NH_2)_2$ (space group $P\bar{4}2_1m$, $Z = 2$(2 mm)) is another example of ELF helping to understand the spatial organization of a crystal. The structure of urea consists of ribbons of doubly hydrogen-bonded molecules arranged in a head-to-tail fashion along the c axis. The plane of each ribbon is perpendicular to the adjacent ribbons oppositely directed along the c axis, the oxygen atom of a carbonyl group in one ribbon is also involved in H-bonds with two adjusted ribbons (Fig. 4a). Intra-ribbon distance O···H measured by the low-temperature neutron diffraction is 2.071(2) Å, while inter-ribbon O···H distance is 2.014(2) Å [32], the longer H-bond being characterized by the lower electron density value at the bond critical point [33]. The ELF pattern presented in Fig. 4b exhibits the details of H-bonding in urea. Oxygen atom has four non-bonding ELF attractors: two of them ($\eta = 0.83$) lay in the plane of a molecule, while the other two ($\eta = 0.79$) belong to the perpendicular plane. All these attractors point towards the ELF holes in the electron shell of the hydrogen atoms behind the nuclei (these holes do not exist in a single molecule). That forms the basis of the three-dimensional H-bonding system in urea, which has a directional key-and-lock character in agreement with the pattern of intermolecular interaction lines in the electron density.

Fig. 4b reveals also an interesting feature of intermolecular interaction in urea: ELF indicates the presence of two non-bonding charge concentrations in the valence shells of the C atoms ($\eta = 0.81$), which also point towards the ELF holes behind the H nuclei in molecules belonging to the two adjacent ribbons. Such an arrangement should result in some secondary attractive interaction between the corresponding molecules, and may be responsible for the mentioned difference between the lengths of the hydrogen bonds. Since there is no corresponding interaction line in the electron density, this interaction is likely to have an electrostatic nature.

3. Conclusion

Suggested modification of the ELF based on the density functional approach significantly expands the framework of the accurate X-ray diffraction analysis. It is now possible to establish the architecture features of whole crystal connected with the electron pair localization (e.g., the nature of the molecular recognition in the solid state). Being combined with standard topological analysis, this approach allows to get the detailed picture of the electron interactions in a crystal compatible with a quantum mechanical description.

All calculations in this work were done with the program WINXPRO [34].

Acknowledgements

The authors thank Professor R.F.W. Bader and Professor A. Savin for reading the manuscript and valuable advices.

References

[1] A.D. Becke, K.E. Edgecombe, J. Chem. Phys. 92 (1990) 5397.
[2] A. Savin, A.D. Becke, J. Flad, R. Nesper, H. Press, H.G. von Schnering, Angew. Chem. Int. Ed. Engl. 30 (1991) 409.
[3] A. Savin, A.D.O. Jepsen, J. Flad, O.K. Andersen, H. Press, H.G. von Schnering, Angew. Chem. Int. Ed. Engl. 31 (1992) 187.
[4] B. Silvi, A. Savin, Nature 371 (1994) 63.
[5] R.F.W. Bader, S. Johnson, T. H. Tang, P.L.A. Popelier, J. Phys. Chem. 100 (1996) 15398.
[6] M. Kohout, A. Savin, Int. J. Quant. Chem. 60 (1996) 85.
[7] A. Savin, R. Nesper, S. Wengert, T.F. Faessler, Angew. Chem. Int. Ed. Engl. 36 (1997) 1808.
[8] V.G. Tsirelson, R.P. Ozerov, Electron Density and Bonding in Crystals: Theory and Diffraction Experiments in Solid State Physics and Chemistry, Institute of Physics, Bristol, Philadelphia, 1996.
[9] R. McWeeny, B.T. Sutsliffe, Methods of Molecular Quantum Mechanics, Academic Press, London, 1976.
[10] R.F.W. Bader, Atoms in Molecules A Quantum Theory, Oxford University Press, Oxford, 1990.
[11] Y. Tal, R.F.W. Bader, Int. J. Quant. Chem. Symp. 12 (1978) 153.
[12] N.H. March, Phys. Lett. A 113 (1986) 476.
[13] M. Levy, H. Ou Yang, Phys. Rev. A 38 (1988) 625.
[14] D.A. Kirzhnits, Sov. Phys. JETP 5 (1957) 64.
[15] R.G. Parr, W. Yang, Density Functional Theory of Atoms and Molecules, Oxford University Press, New York, 1989.
[16] M. Hoffmann Ostenhof, T. Hoffmann Ostenhof, Phys. Rev. A 16 (1977) 1782.
[17] V.G. Tsirelson, M.V. Yakovlev, Russ. J. Phys. Chem., submitted.
[18] V.G. Tsirelson, Yu. V. Ivanov, in: Sagamore XIII. Conference on the Charge, Spin and Momentum Densities, Book of Abstracts, Institute of Experimental Physics, 2000, p. 104.
[19] C.F v. Weizsacker, Z. Phys. 96 (1935) 431.
[20] W. Yang, Phys. Rev. A 34 (1986) 4575.
[21] P. Fuentealba, Int. J. Quant. Chem. 69 (1998) 559.
[22] R.J. Gillespie, I. Hargittai, The VSEPR Model of Molecular Geometry, Prentice Hall, Englewood Cliffs, NJ, 1991.
[23] J. Lennard Jones, J. Chem. Phys. 20 (1952) 1024.
[24] R.J. Gillespie, D. Bayes, J. Platts, G.L. Heard, R.F.W. Bader, J. Phys. Chem. A 102 (1998) 3407.
[25] R.F.W. Bader, M.E. Stephens, Chem. Phys. Lett. 26 (1974) 445.
[26] R.F.W. Bader, M.E. Stephens, J. Am. Chem. Soc. 97 (1975) 7391.
[27] X. Krokidis, N.W. Moriarty, W.A. Lester, M. Frenklach, Chem. Phys. Lett. 314 (1999) 534.
[28] H. Chevreau, A. Sevin, Chem. Phys. Lett. 322 (2000) 9.
[29] E.D. Stevens, Mol. Phys. 37 (1979) 27.
[30] V.G. Tsirelson, P.F. Zou, T. H. Tang, R.F.W. Bader, Acta Cryst. A 51 (1995) 143.
[31] M. Tafipolsky, W. Scherer, V.Tsirelson, to be published.
[32] S. Swaminathan, B.M. Craven, R.K. McMullan, Acta Cryst. B 40 (1984) 300.
[33] V.E. Zavodnik, A.I. Stash, V.G. Tsirelson, R.Y. de Vries, D. Feil, Acta Cryst. B 55 (1999) 45.
[34] A. Stash, V. Tsirelson, WinXPRO A Program for Calculation of the Crystal and Molecular Properties Using the Model Electron Density, 2001 <http://stash.chat.ru>.